

Mechanism of Yi-Qi-Bu-Shen Recipe for the Treatment of Diabetic Nephropathy Complicated with Cognitive Dysfunction Based on Network Pharmacology and Experimental Validation

Wenyi Li^{1,2}, Zhenguo Liu¹, Min Song¹, Zhenpeng Shi¹, Jihang Zhang³, Junyu Zhou¹, Yidan Liu¹, Yun Qiao⁴, Deshan Liu⁴

¹First Clinical Medical College, Shandong University of Traditional Chinese Medicine, Jinan, People's Republic of China; ²Research Center for Basic Medical Sciences, Qilu Hospital of Shandong University, Jinan, People's Republic of China; ³Traditional Chinese Medicine College, Shandong University of Traditional Chinese Medicine, Jinan, People's Republic of China; ⁴Department of Traditional Chinese Medicine, Qilu Hospital of Shandong University, Jinan, People's Republic of China

Correspondence: Deshan Liu, Department of Traditional Chinese Medicine, Qilu Hospital of Shandong University, Jinan, Shandong, 250012, People's Republic of China, Tel +86 18560087381, Email liudeshan@sdu.edu.cn

Context: Diabetic nephropathy (DN) and cognitive dysfunction (CD) are common complications of diabetes. Yi-Qi-Bu-Shen Recipe (YQBS) can effectively reduce blood glucose, improve insulin resistance, and delay the progression of diabetic complications. The underlying mechanisms of its effects need to be further studied.

Objective: This study elucidates the mechanism of YQBS in DN with CD through network pharmacology and experimental validation.

Materials and Methods: Protein-protein interaction, Gene Ontology (GO), and Kyoto Encyclopedia of Genes and Genomes (KEGG) enrichment analyses were performed. Male Sprague-Dawley (SD) rats were divided into 6 groups: model, YQBS (2, 4, 8 g/kg), positive control (metformin, 200 mg/kg), and control; the DN model was established by high sugar and high fat diet combined with intraperitoneal streptozotocin injection. After the DN model was established, the rats were gavaged for 10 weeks. Serum, kidneys, and hippocampus tissues were collected to measure the expression levels of TLR4, NF- κ B, TNF- α , and IL-6.

Results: The network pharmacology analysis showed that quercetin and kaempferol were the main active components of YQBS. TNF and IL-6 were the key targets, and TLR4/NF- κ B pathway was crucial to YQBS in treating DN complicated with CD. Experimental validation showed that the intervention of YQBS can reduce TNF- α and IL-6 in serum, and also significantly decreases the protein expression of TLR4 and NF- κ B.

Conclusion: YQBS exerts anti-inflammatory effects on DN with CD through TLR4/NF- κ B pathway. This study provides a biological basis for the scientific usage of YQBS in inflammation diseases and supplies experimental evidence for future traditional Chinese medicine development.

Keywords: Yiqi Bushen Recipe, diabetes nephropathy, cognitive dysfunction, network pharmacology, inflammation

Introduction

As a common endocrine metabolic disorder caused by multiple factors, diabetes mellitus (DM) is a complex disease driven by various pathological and physiological processes. It is characterized by chronic hyperglycemia, which can lead to chronic damage and dysfunction in various organs.¹ Currently, DM has become one of the world's public health problems that seriously threaten human health. Diabetic nephropathy (DN) is one of the most prevalent microvascular complications of DM, playing a crucial role in chronic renal failure and end-stage renal disease.² About 30% to 40% of DM patients are at risk of developing DN, with a high likelihood of progressing to end-stage renal disease; moreover, the 5-year survival rate for end-stage renal disease patients is typically below 20%.³ Cognitive dysfunction (CD) is not

uncommon among individuals with DM. In the 1920s, Miles and Root first suggested the presence of CD in DM. Numerous epidemiological studies have shown that there is a relationship between diabetes and cognitive impairment.⁴ The metabolic disruptions triggered by hyperglycemia can induce damage to the central nervous system, resulting in cognitive impairment.^{5–7} In clinical practice, DN patients may have different degrees of CD. The precise mechanism underlying the combination of DN and CD remains somewhat unclear, garnering significant attention from scholars in recent years. Research has indicated that in individuals with type 2 diabetes and glycosylated hemoglobin >7.5% and a high risk of cardiovascular disease, cognitive decline is related to DN.⁸ One explanation for the association between kidney disease and cognitive impairment may lie in the similar hemodynamics of the kidneys and brain. Both microcirculatory systems are characterized by low resistance and are exposed to high circulating flow, making them more susceptible to vascular damage.^{9,10} CD in DM patients is like the microvascular lesions observed in kidney impairment, manifesting as thickening of the capillary basement membrane, lumen narrowing, vascular endothelial dysfunction, and increased vascular permeability, etc. Vascular endothelial dysfunction-induced impairment of self-regulation may elevate pressure within the two circulatory systems, leading to organ damage.^{11,12} At present, the treatment of DN and CD primarily involves a comprehensive approach focused on reducing blood sugar, blood pressure, and lipid levels, alongside symptomatic therapies. Multiple studies have indicated that exaggerated expressions of Toll-like receptor 4 (TLR4) and NF- κ B are positively associated with the progression of DN and CD, while proinflammatory factors like interleukin-6 (IL-6) as well as tumor necrosis factor (TNF) are closely correlated with DN and CD.^{13–16}

Traditional Chinese medicine (TCM) believes that DN, known as “Xiaoke” in Chinese, can be attributed to Shenqi deficiency leading to functional disorders.¹⁷ Yi-Qi-Bu-Shen Recipe (YQBS) was derived from the classic formula Shen-Qi-Di-Huang decoction with modifications, focusing on tonifying qi and kidney, promoting blood circulation, and resolving phlegm. Shen-Qi-Di-Huang decoction was first recorded in the classical Chinese medicine book “Identify the Origins of Miscellaneous Diseases” (Zabing Yuanliu Xizhu). This decoction targets syndromes related to qi and yin deficiency, as well as kidney deficiency, exhibiting significant therapeutic effects in treating DN.^{18–21} YQBS consists of nine ingredients of TCM, including the root of *Astragalus membranaceus* Fisch. [Fabaceae] (HQ; Pinyin name Huangqi), the rhizome of *Rehmannia glutinosa* Libosch. [Orobanchaceae] (SD; Pinyin name Shudihuang), the rhizome of *Polygonatum sibiricum* Red. [Asparagaceae] (HJ; Pinyin name Huangjing), the rhizome of *Ligusticum chuanxiong* Hort. [Apiaceae] (CX; Pinyin name Chuanxiong), the mature fruit of *Lycium barbarum* L. [Solanaceae] (GQZ; Pinyin name Gouqizi), the leaf of *Epimedium brevicornu* Maxim. [Berberidaceae] (YYH; Pinyin name Yinyanghuo), the rhizome of *Atractylodes lancea* DC. [Asteraceae] (CZ; Pinyin name Cangzhu), the root of *Pueraria lobata* (Willd). Ohwi [Fabaceae] (GG; Pinyin name Gegen), and the rhizome of *Coptis chinensis* Franch. [Ranunculaceae] (HL; Pinyin name Huanglian). Previous studies conducted by our team have demonstrated that YQBS can delay the progression of DM and its associated complications.^{22,23} Evidence suggests that YQBS (formerly known as NaoShenKang Capsule) can ameliorate diabetes symptoms and complications in DM patients.²⁴ Animal experiments also demonstrated that YQBS could effectively improve renal function, mitigate kidney pathological changes, and alleviate renal inflammation and fibrosis.^{25,26} Furthermore, our results in previous research indicated that YQBS might improve CD in diabetic rats by enhancing the antioxidant activity of neurons, inhibiting apoptosis, and alleviating the damage of hippocampal neurons.^{27,28}

In conclusion, the mechanism by which YQBS improves DN complicated with CD remains unclear. Therefore, this study used network pharmacology and experimental validation to explore the possible targets and mechanisms of YQBS in treating DN combined with CD.

Materials and Methods

Network Pharmacology Analysis

Screening for Active Components in YQBS and Target Prediction

The Traditional Chinese Medicine Systems Pharmacology Database and Analysis Platform (TCMSP, <https://tcmsp.com/tcmssp.php>)²⁹ is a pharmacological database of Chinese herbal medicine that includes a network of targets for drugs, chemicals, targets, and diseases, along with the pharmacokinetic characteristics of compounds such as oral bioavailability (OB) and drug likeness (DL).³⁰ The compounds of YQBS were acquired from TCMSP, with OB \geq 30% alongside DL \geq 0.18 serving as the

screening criteria.³¹ The corresponding targets of the active ingredients within YQBS were predicted by TCMSP. The UniProt database (<https://www.uniprot.org/>)³² was adopted to standardize the target names of YQBS active ingredients into gene names. The visualization of YQBS compound-target network was achieved using Cytoscape 3.9.1.

Screening for Disease Related Targets

The potential targets of DN (search term “diabetic nephropathy”) and CD (search term “cognitive dysfunction”) were searched from the five databases: OMIM (<https://www.omim.org/>),³³ GeneCards (<https://www.genecards.org/>),³⁴ DrugBank (<https://go.drugbank.com/>),³⁵ DisGeNET (<https://www.disgenet.org/>),³⁶ and TTD (<http://db.idrblab.net/ttd/>).³⁷

Prediction of YQBS Targets for DN with CD Treatment

The overlapping targets of YQBS, DN, and CD were identified using Venny 2.1.0, and the drug-disease-target network was visualized using Cytoscape.

Construction of Protein–Protein Interaction (PPI) Network

The shared targets of drugs and diseases were imported into the STRING database (<https://string-db.org/>)³⁸ to construct a PPI network. The CytoNCA plugin in Cytoscape 3.9.1 was used to calculate the parameters of nodes: betweenness centrality (BC), closeness centrality (CC), degree centrality (DC), eigenvector centrality (EC), network centrality (NC), and local average connectivity (LAC). A node’s importance in the network increases with a higher parameter value. The node data were sieved based on the average of these six parameters, and nodes surpassing the average were considered key targets.³⁹ PPI networks for both total and key targets were constructed using Cytoscape.

Enrichment Analysis

The key targets were imported into the DAVID database (<https://david.ncifcrf.gov/>)⁴⁰ for Gene Ontology (GO) enrichment analysis. The species “Homo sapiens” was selected to examine biological processes (BP), cellular components (CC), as well as molecular functions (MF) related to the intervention of YQBS in the merging of DN and CD. Metascape (<https://metascape.org/>)⁴¹ was utilized for Kyoto Encyclopedia of Genes and Genomes (KEGG) pathway enrichment analysis. The bioinformatics online platform (<https://www.bioinformatics.com.cn/>), an online platform for data analysis and visualization to create bubble diagrams and signal pathway diagrams, was used for visualization.

Construction of Drug-Target-Pathway Network

The primary active compounds of YQBS, key targets, and main signaling pathways were imported into Cytoscape 3.9.1 to construct a drug-target-pathway network, to examine the potential mechanisms of YQBS in treating DN with CD.

Molecular Docking

The 2D structures of the main active ingredients of YQBS were obtained from the PubChem website (<https://pubchem.ncbi.nlm.nih.gov/>).⁴² Subsequently, they were converted into 3D structures through Chem3D software. The protein structures of the key targets were downloaded from the PDB database (<https://www.rcsb.org/>).⁴³ Molecular docking was conducted through Autodock Vina and PyMol.⁴⁴

Experimental Validation

Reagents

Streptozotocin (STZ, IS0250) and 0.1 mol/L Sodium Citrate buffer (C1013) were bought from Beijing Solarbio Science & Technology Co. (Beijing, China). The primary antibodies used were as follows: TLR4 (A21626) was purchased from ABclonal Technology Co. (Wuhan, China); NF- κ B p65 (WL01980) and phospho-NF- κ B p65 (WL02169) were purchased from Shenyang Wanlei Biotechnology Co. (Shenyang, China); β -actin (81115-1-RR) was purchased from Proteintech (Wuhan, China). The horseradish peroxidase (HRP)-conjugated secondary antibodies (SA00001-2) were also purchased from Proteintech. Enzyme-linked immunosorbent assay (ELISA) kits for Urinary microalbumin (ml059011), TNF- α (ml002859), and IL-6 (ml102828) for rats were purchased from Shanghai Enzyme-linked Biotechnology Co. (Shanghai, China).

Animals

Thirty-six 6-week-old male Sprague Dawley rats were purchased from Jinan Pengyue Experimental Animal Breeding Co. (Jinan, China). All animals were kept in the specific pathogen-free room at the Laboratory Animal Center of Qilu Hospital of Shandong University (Shandong, China) with a 12 h light/dark cycle. All rats and experimental protocol were approved by the Experimental Animal Ethics Committee of Qilu Hospital of Shandong University (DWLL-2022-073).

Preparation of YQBS Recipe

In this study, the nine herbs (30 g HQ, 24 g SD, 20 g HJ, 12 g CX, 12 g GQZ, 18 g YYH, 10 g CZ, 24 g GG, 6 g HL) in YQBS were sourced from the pharmacy of Qilu Hospital, and all were included in the Chinese Pharmacopoeia. The herbs were authenticated by Professor Lihong Zhong. Voucher specimen (T001700368, T001700710, T001700444, T001200132, T001700294, T001700850, T000500258, T000100286, T000200367) was preserved in Qilu Hospital. The herbs mentioned above were decocted and extracted three times with total 20 times the amount of water (added approximately 3100 mL of water to 156 g herbs) at 100°C, each time for 2 h. The resulting decoction liquid was combined, filtered, concentrated to a thick paste, transferred to a vacuum drying oven (80°C) for drying, ground into a powder, and stored in a refrigerator at 4°C for future use. The quality control of YQBS was established.⁴⁵ Each gram of YQBS dried Chinese medicine powder corresponded to 3.564 g of crude medicine.

Ultra-Performance Liquid Chromatography Tandem Mass Spectrometry (UPLC-MS/MS) Analysis

The components analysis of YQBS was conducted using Ultra Performance Liquid Chromatography (SCIEX ExionLC™ AD). The YQBS dry powder of TCM was dissolved in a liquid. A 100 µL YQBS liquid sample was placed into a 1.5 mL sterile centrifuge tube, and 100 µL of pre-cooled 70% methanol containing internal standard extraction solution was added, then vortexed for 15 min. Following centrifugation at 12000 rpm, 4°C for 3 min, the supernatant was filtered through a 0.22 µm pore size microporous filter for further testing. Chromatographic analysis was carried out on an SB-C18 chromatographic column at a temperature of 40°C, with a flow rate of 0.35 mL/min and an injection volume of 2 µL. Phase A consisted of 0.1% formic acid ultrapure water, while Phase B comprised 0.1% formic acid acetonitrile. The gradient elution procedure was as follows: at 0 min, the proportion of Phase B was 5%, which linearly increased to 95% within 9 min and was maintained at 95% for 1 min. Subsequently, the proportion of Phase B decreased to 5% within 1 min and was held at 5% for an additional 14 min for equilibrium. Mass spectrometry analysis was performed using the AB 6500 QTRAP mass spectrometer.

Construction of Experimental DN Model and Grouping

Rats were randomly divided into 6 groups, each consisting of 6 rats: the model group (DN), YQBS low-dose group (YQBS-L), YQBS medium-dose group (YQBS-M), YQBS high-dose group (YQBS-H), metformin group (Metformin), and control group (Control). Except the Control group, rats were fed a high-sugar and high-fat diet for 6 weeks and intraperitoneally injected with 35 mg/kg of STZ.^{46,47} Successful diabetes modeling was confirmed after 72 h when random blood glucose levels were ≥ 16.7 mmol/L for 3 consecutive days. Following 6 weeks of the high-sugar and high-fat diet, 24 h urine samples were collected. DN modeling was confirmed based on criteria including urine volume greater than 150% of normal, presence of urine sugar, and 24 h urinary albumin exceeding 30 mg. The dosages of YQBS and metformin administered to the rats were determined based on clinical dosages and equivalent conversion between human and rat dosages, with a conversion ratio of 6.3. The YQBS groups received daily gavage of YQBS at doses of 2, 4, and 8 g/kg, while the metformin group received daily gavage of 200 mg/kg metformin. Metformin hydrochloride tablets were provided by Bristol Myers Squibb Co. Rats in either the DN group or the Control group were administered an equal volume of normal saline. The rats' fur, water and food intake, mental state, urine, and feces were observed daily, and their weight and blood sugar were measured every 4 weeks. After 10 weeks of continuous gavage, Morris water maze (MWM) test was carried out and 24 h urine samples were collected. Subsequently, the blood, kidney, and brain tissues of rats were collected for subsequent analysis.

Morris Water Maze (MWM) Experiment

MWM was adopted to examine the learning and memory function of experimental rats. The water maze was composed by a cylindrical stainless steel pool with a black inner wall, with a diameter of 150 cm and a height of 50 cm. Clean water was filled in the pool to a depth of 25 cm, with the water temperature maintained between 22–25°C. A black solid circular platform with a diameter of 10 cm, was placed in the maze, submerged 1 cm below the water surface and capable of movement. A monitoring system connected to a computer was positioned above the pool. The surroundings of the pool were kept constant, with stable lighting and a quiet environment. Following 10 weeks of gavage administration, the experimental rats began to undergo MWM adaptation training at a frequency of 4 times a day, each lasting for 120s. The water surface was divided into four quadrants, with the platform placed in the center of one quadrant. Rats were placed in the water within one quadrant to search for the platform. When a rat successfully reached the platform, the computer would cease tracking and automatically calculate the time taken for the rat to locate the platform (latency period). If a rat reached the platform within 120s, it would be permitted to stay on it for an additional 15s. However, if a rat failed to reach the platform within 120s, it would be guided to the platform and permitted to stay for an additional 15s, with the latency recorded as 120s. After training for 5 days, the rats were placed in the water within one quadrant, with the platform removed on the 6th day. The number of times and the duration for which the rats passed through the area where the platform had been located were recorded within 120s. The data collected during these experiments were recorded using Topscan Version.

Histopathological Analysis

After collecting 24 h urine and MWM test, rats were intraperitoneal injected of sodium pentobarbital to minimize suffering. The samples of brain tissues were subjected to fixation in 4% paraformaldehyde (Biosharp, BL539A) for a period of 24 h, dehydrated, and embedded in paraffin. Subsequently, they were sectioned in the coronal plane, each with 5 μ m in thickness, and stained with hematoxylin and eosin (H&E).

Enzyme-Linked Immunosorbent Assay (ELISA)

The serum levels of TNF- α as well as IL-6 were determined following the instructions provided with the ELISA kits.

Western Blotting

Total protein from kidneys and hippocampus tissues was extracted using a whole protein extraction kit (Solarbio, BC3710). The bicinchoninic acid (BCA) protein quantification kit (Share-Bio, SB-WB013) was used to quantify the protein levels. Sodium dodecyl sulfate polyacrylamide gel electrophoresis (SDS-PAGE) was used to separate proteins from the kidneys and hippocampus, which were then transferred to 0.2 μ m polyvinylidene fluoride (PVDF) membranes (Immobilon[®]-P^{SQ}, ISEQ00010). The membranes were sealed with a rapid sealing solution (Servicebio, G2052-500ML) for 15 min at room temperature and subsequently incubated overnight at 4°C with primary antibodies. The dilution ratios for TLR4, NF- κ B p65, and phospho-NF- κ B p65 were 1:500, 1:2000, and 1:1000, respectively. Subsequently, the membranes were subjected to incubation with secondary antibodies at room temperature and then exposed to a chromogenic solution.

Statistical Analysis

All results were presented as mean \pm standard error of the mean (SEM). Multiple group comparisons were conducted using one-way analysis of variance (ANOVA). Data processing and analysis were conducted using GraphPad Prism 8.0 software. A p-value of less than 0.05 was considered statistically significant.

Results

Network Pharmacology Analysis

Active Ingredients and Targets of YQBS

By searching the TCMSP database, a total of 120 active ingredients of YQBS were identified, including 20 active compounds of HQ, 2 active compounds of SD, 12 active compounds of HJ, 7 active compounds of CX, 45 active compounds of GQZ, 23 active compounds of YYH, 9 active compounds of CZ, 4 active compounds of GG, and 14 active compounds of HL. Different

drugs in YQBS contain the same active ingredients, with 11 duplicate ingredients, as detailed in Table 1. According to Cytoscape 3.9.1 analysis, 24 active ingredients exhibited a degree value of ≥ 20 (Table 2), mainly including quercetin, kaempferol, β -sitosterol, formaronetin, stigmasterol, luteolin, and wogonin.

The potential targets for active ingredients were retrieved from the TCMSP database and then standardized into gene names using the UniProt database. In total, 1011 targets of YQBS were identified, with 197 from HQ, 30 from SD, 81 from HJ, 25 from CX, 189 from GQZ, 208 from YYH, 53 from CZ, 59 from GG, and 169 from HL. Following the removal of duplicates, a total of 248 different targets were identified. The active ingredients of YQBS and their potential targets were integrated into Cytoscape for the construction of the compound-target network (Figure 1A).

Table 1 Information on Repetitive Active Ingredients of YQBS

Number	Mol ID	Molecule name	OB%	DL	Drug
A1	MOL000098	Quercetin	46.43	0.28	HQ, GQZ, YYH, HL
A2	MOL000359	Sitosterol	36.91	0.75	SD, HJ, CX, YYH
B	MOL000358	Beta-sitosterol	36.91	0.75	HJ, GQZ, GG
C1	MOL000433	FA	68.96	0.71	HQ, CX
C2	MOL000422	Kaempferol	41.88	0.24	HQ, YYH
C3	MOL000392	Formononetin	69.67	0.21	HQ, GG
C4	MOL000449	Stigmasterol	43.83	0.76	SD, GQZ
C5	MOL001792	DFV	32.76	0.18	HJ, YYH
C6	MOL002959	3'-Methoxydaidzein	48.57	0.24	HJ, GG
C7	MOL001494	Mandenol	42.00	0.19	CX, GQZ
C8	MOL000622	Magnograndiolide	63.71	0.19	YYH, HL

Table 2 Information on the Main Effective Components of YQBS

Number	Mol ID	Molecule name	OB%	DL	Degree
A1	MOL000098	Quercetin	46.43	0.28	574
C2	MOL000422	Kaempferol	41.88	0.24	117
B	MOL000358	Beta-sitosterol	36.91	0.75	99
C3	MOL000392	Formononetin	69.67	0.21	66
C4	MOL000449	Stigmasterol	43.83	0.76	62
YYH18	MOL000006	Luteolin	36.16	0.25	55
CZ1	MOL000173	Wogonin	30.68	0.23	41
HQ7	MOL000378	7-O-methylisomucronulatol	74.69	0.30	39
YYH8	MOL004380	C-Homoerythrinan, 1,6-didehydro-3,15,16-trimethoxy-, (3.beta.)-	39.14	0.49	38
HJ1	MOL002714	Baicalin	33.52	0.21	34
YYH7	MOL004373	Anhydroicaritin	45.41	0.44	33
C6	MOL002959	3'-Methoxydaidzein	48.57	0.24	32
HQ5	MOL000354	Isorhamnetin	49.60	0.31	31
HL4	MOL002903	(R)-Canadine	55.37	0.77	28
GQZ27	MOL009650	Atropine	42.16	0.19	28
YYH13	MOL004391	8-(3-methylbut-2-enyl)-2-phenyl-chromone	48.54	0.25	27
GQZ5	MOL005406	Atropine	45.97	0.19	26
YYH5	MOL003542	8-Isopentenyl-kaempferol	38.04	0.39	24
CX1	MOL002135	Myricanone	40.60	0.51	22
C5	MOL001792	DFV	32.76	0.18	22
HQ6	MOL000371	3,9-di-O-methylnisolin	53.74	0.48	21
HQ3	MOL000296	Hederagenin	36.91	0.75	21
CZ3	MOL000188	3 β -acetoxyatractylone	40.57	0.22	20
HQ9	MOL000380	(6aR,11aR)-9,10-dimethoxy-6a,11a-dihydro-6H-benzofurano[3,2-c]chromen-3-ol	64.26	0.42	20

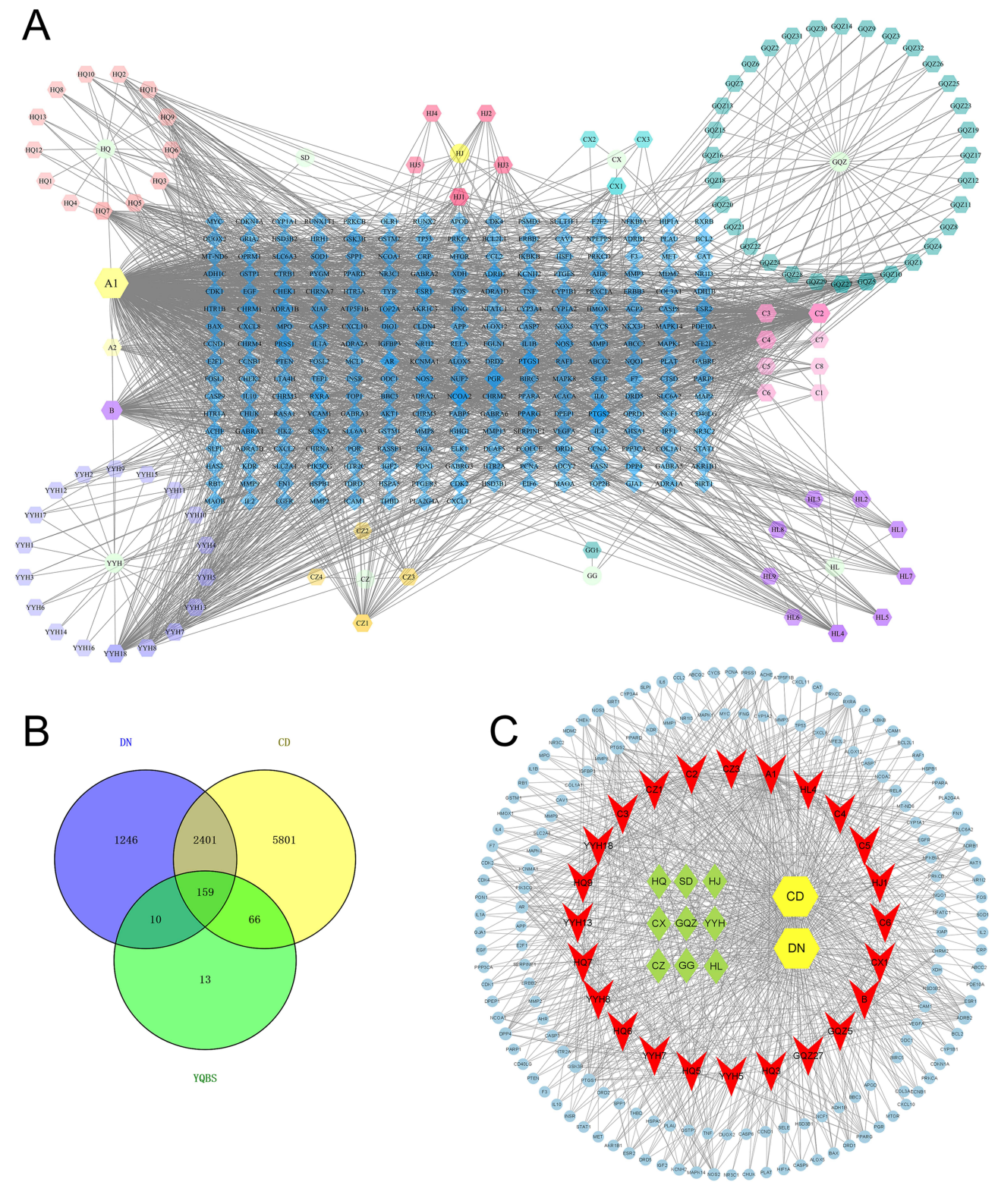


Figure 1 Compound-target network of YQBS and drug-disease target network. **(A)** TCM compounds are depicted as circles, active ingredients as hexagons, and targets as diamonds. HQ: *Astragalus membranaceus*; SD: *Rehmannia glutinosa*; HJ: *Polygonatum sibiricum*; CX: *Ligusticum chuanxiong*; GQZ: *Lycium barbarum*; YYH: *Epimedium brevicornu*; CZ: *Atractylodes lancea*; GG: *Pueraria lobata*; HL: *Coptis chinensis*. A1: Common ingredients of *Astragalus membranaceus*, *Lycium barbarum*, *Epimedium brevicornu*, and *Coptis chinensis*; A2: Common components of *Rehmannia glutinosa*, *Polygonatum sibiricum*, *Ligusticum chuanxiong*, and *Epimedium brevicornu*; B: Common components of *Polygonatum sibiricum*, *Lycium barbarum*, and *Pueraria lobata*; C1-C8: Common components of two types of TCM in YQBS. **(B)** Venn diagram of the intersection targets among YQBS, DN, and CD. **(C)** Drug-disease-target network showing 9 drugs, 24 active compounds, and 159 targets. Targets are represented by circles, drugs by diamonds, and compounds by arrows.

Disease Related Targets

The relevant targets associated with DN and CD were retrieved from five databases: OMIM, GeneCards, DrugBank, DisGeNET, and TTD. Upon merging the data and eliminating duplicates, a total of 3816 targets for DN and 8427 targets for CD were compiled.

Common Targets of YQBS and Diseases

The Venny 2.1.0 platform was utilized to identify 159 common targets shared between YQBS, DN, and CD (Figure 1B). These targets are regarded as potential targets for the treatment of DN and CD with YQBS. Subsequently, the drug-disease-target network was visualized using Cytoscape (Figure 1C).

PPI Network Construction and Core Targets

The 159 targets that are common to both diseases and drugs were input into the STRING platform to obtain a preliminary PPI network, resulting in 159 nodes and 3437 connections (Figure 2A). Subsequently, this network was further refined and visualized using Cytoscape (Figure 2B). The data was analyzed and filtered with DC, BC, CC, EC, NC, as well as LAC in Cytoscape. The intermediate values were 43.2327, 133.3081765, 0.556947093, 0.066241445, 34.1962077, and 26.31310603, respectively. A total of 37 core targets with 613 connections surpassing the intermediate values were identified (Table 3), indicating their significance as key targets of YQBS in treating DN complicated with CD. A refined PPI network was then constructed specifically focusing on these key targets using Cytoscape (Figure 2C).

GO and KEGG Analysis

GO analysis of the 37 core targets was conducted on the DAVID platform, resulting in a total of 534 GO entries, including 435 BPs, 33 CCs, and 66 MFs. The top 10 P-values for BPs, CCs, and MFs were selected for the visualization (Figure 2D). The results showed that the main BPs involved positive regulation of gene expression, angiogenesis, cellular response to hypoxia, and positive regulation of pri-miRNA transcription from RNA polymerase II promoter. In terms of CCs and MFs, the most significant categories were macromolecular complex and enzyme binding, respectively.

Through an examination of the KEGG pathways associated with the core targets, 15 highly probable signaling pathways were enriched using Metascape, as shown in Figure 2E. The treatment of DN complicated with CD using YQBS may be mainly related to signaling pathways such as Human cytomegalovirus infection, HIF-1 signaling pathway, and NF-kappa B signaling pathway.

Drug-Target-Pathway Network Construction

The main compounds of YQBS, intersection targets among drugs, diseases and main signal pathways were constructed using Cytoscape (Figure 3). The network among the main active ingredients of YQBS, signal pathways, and key targets was displayed.

Molecular Docking

TNF and IL-6 were identified as core targets. The most significant active components in YQBS were quercetin and kaempferol, with binding energies less than -5.0 kcal/mol, as shown in Table 4. The binding of TNF to quercetin and kaempferol was shown in Figure 4.

Based on the comprehensive analysis of the drug-target-pathway network, PPI network, GO and KEGG analysis, it is suggested that YQBS may exert its beneficial effects on DN combined with CD through four key targets: TLR4, NF-kB, TNF- α , and IL-6.

Experimental Validation

Identification of the Chemical Composition of YQBS

We used the UPLC-MS/MS method to analyze the main components of YQBS. The total ion chromatograms of YQBS are shown in Figure 5A and B. A total of 1061 metabolites were detected, including quercetin, kaempferol, formononetin, luteolin, wogonin, baicalein, anhydroicaritin, 3'-methoxydaidzein, isorhamnetin, canadine, and other components. These 10 components are ranked in the top 15 in Table 2, indicating that the active ingredients predicted by TCMSP are relatively reliable.

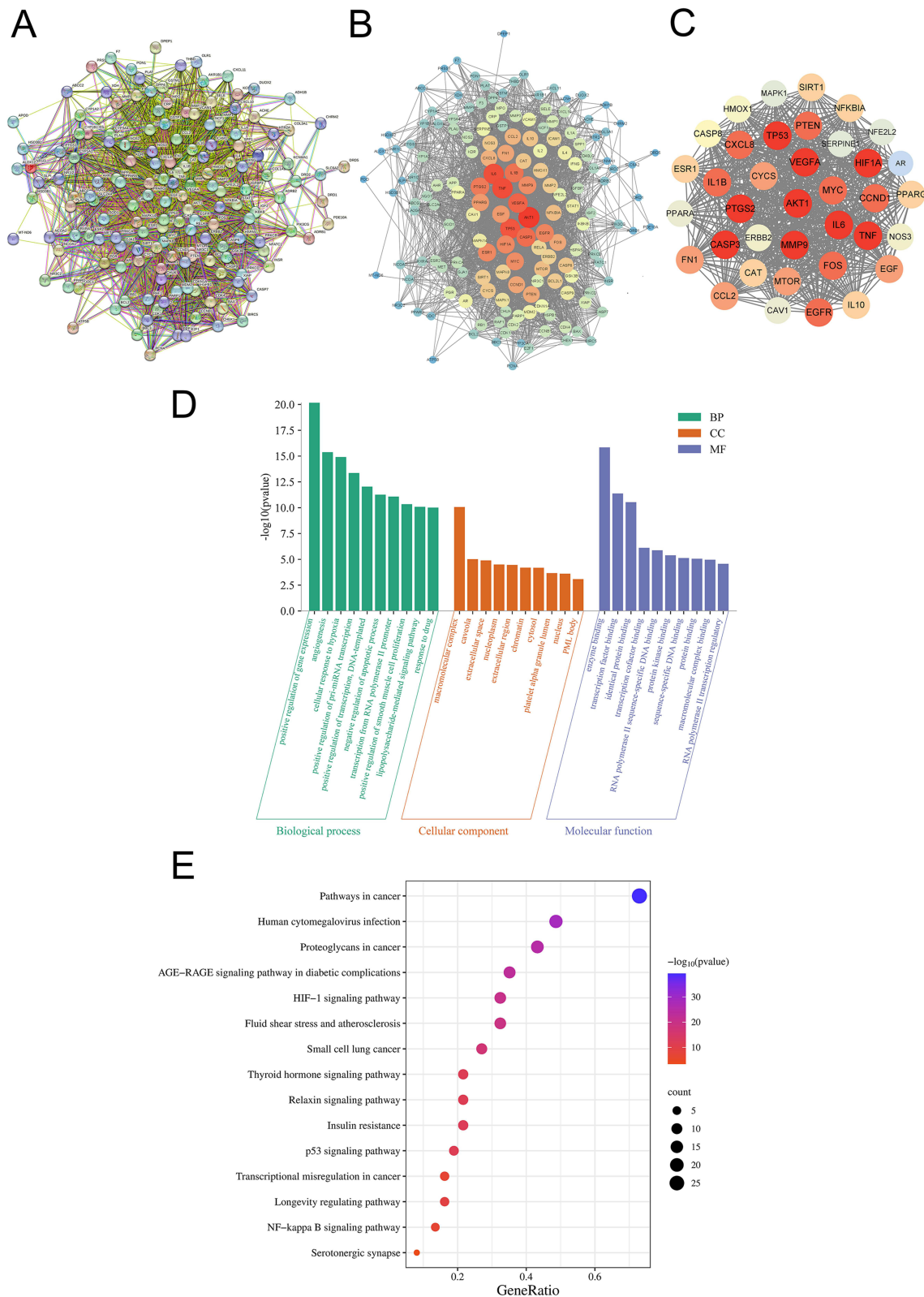


Figure 2 PPI network, GO functional, and KEGG pathway enrichment analysis. **(A)** PPI network of YQBS targets for treating DN with CD from STRING. **(B)** PPI network processed using Cytoscape. **(C)** PPI network of 37 core targets selected from **(B)** based on DC, BC, CC, EC, NC, and LAC. **(D)** Top 10 P-values for BPs, CCs, and MFs. **(E)** Top 15 signaling pathways identified from KEGG analysis. Drug-target-pathway network construction.

Table 3 Core Targets Information

Target	DC	BC	CC	EC	NC	LAC
AKT1	121	1401.4208	0.810256	0.156645	112.1419	47.3058
TNF	115	897.0245	0.782178	0.152757	104.5397	47.3565
IL6	114	875.6893	0.778325	0.151711	103.3564	47.2807
TP53	112	705.0456	0.763285	0.152935	102.7334	49.1429
VEGFA	107	482.1823	0.745283	0.151626	97.7473	50.3364
CASP3	104	427.1863	0.734883	0.149391	94.0274	50.4615
IL1B	102	509.8609	0.731482	0.142439	89.5372	47.1765
PTGS2	99	584.3077	0.714932	0.141704	85.6272	47.8384
EGFR	96	625.1819	0.711712	0.136019	79.4287	45.5417
ESR1	95	560.9489	0.699115	0.131861	78.6003	44.4211
HIF1A	95	285.2815	0.699115	0.141543	82.8905	49.9789
MMP9	93	392.2750	0.696035	0.137942	81.4325	48.7957
MYC	93	307.1026	0.699115	0.136779	79.9788	48.2581
PPARG	89	404.0186	0.692982	0.128665	70.3149	43.9775
EGF	89	268.5411	0.681035	0.134618	75.1508	48.4045
FNI	85	282.0824	0.675213	0.127645	70.3549	46.0941
CCND1	85	230.0362	0.669492	0.128279	71.2688	47.0118
FOS	84	708.2946	0.672340	0.125841	65.6675	44.8095
PTEN	84	240.8928	0.669492	0.127022	70.3013	47.0238
CXCL8	81	214.0638	0.661088	0.124012	66.4709	46.0988
CCL2	80	199.8785	0.655602	0.121083	66.9136	45.5250
NFKBIA	77	146.1195	0.644898	0.123431	62.4466	47.5065
MTOR	77	141.9078	0.650206	0.120847	62.8353	46.4156
IL10	75	140.5058	0.637097	0.118467	61.5691	45.8933
CASP8	74	148.4902	0.637097	0.117649	59.6520	45.5946
CAT	74	432.1370	0.644898	0.110440	55.9142	40.3243
CYCS	73	520.2894	0.637097	0.112130	55.4429	42.0548
NOS3	73	349.3281	0.642276	0.105965	54.1869	38.1370
SIRT1	72	156.1687	0.637097	0.112485	54.3675	42.3889
HMOX1	72	192.8306	0.632000	0.111129	54.7792	41.9722
ERBB2	70	150.1378	0.634538	0.109170	53.0383	41.3429
MAPK1	65	398.3240	0.619608	0.099541	47.7242	37.8462
CAVI	62	372.5235	0.610039	0.093273	42.9176	33.6774
AR	60	350.5487	0.603053	0.087089	41.9203	32.9000
SERPINE1	59	173.1001	0.598485	0.090501	45.5669	36.3390
PPARA	58	146.3238	0.605364	0.089836	39.4867	33.5172
NFE2L2	53	144.5476	0.585185	0.085755	38.6843	33.9623

Protective Effect of YQBS on DN Combined with CD in Rats

After YQBS treatment, the weight loss caused by diabetes was reduced to some extent (Figure 6A). The fasting blood glucose (FBG) and 24 h urinary microalbumin concentration (mALB) in the YQBS groups were significantly decreased compared to the DN group (Figure 6B and C), indicating an improvement in renal and pancreatic function.

Besides, the protective effect of YQBS on hippocampal neurons in DN rats was obvious. In the Control group, the hippocampal tissue structure was intact, with a regular arrangement, uniform distribution, clear outline of nerve cells, and round and compact nuclei. In the DN rats, the hippocampal tissue structure was damaged, with disordered arrangement of nerve cells, a sharp reduction in number, abnormal shapes, large gaps, and unclear contours. Following the intervention of YQBS and Metformin, the hippocampal tissue structure of the rats gradually recovered, and the degree of morphological damage to nerve cells significantly improved. The arrangement became relatively orderly, with no significant difference among the various treatment groups (Figure 6D).

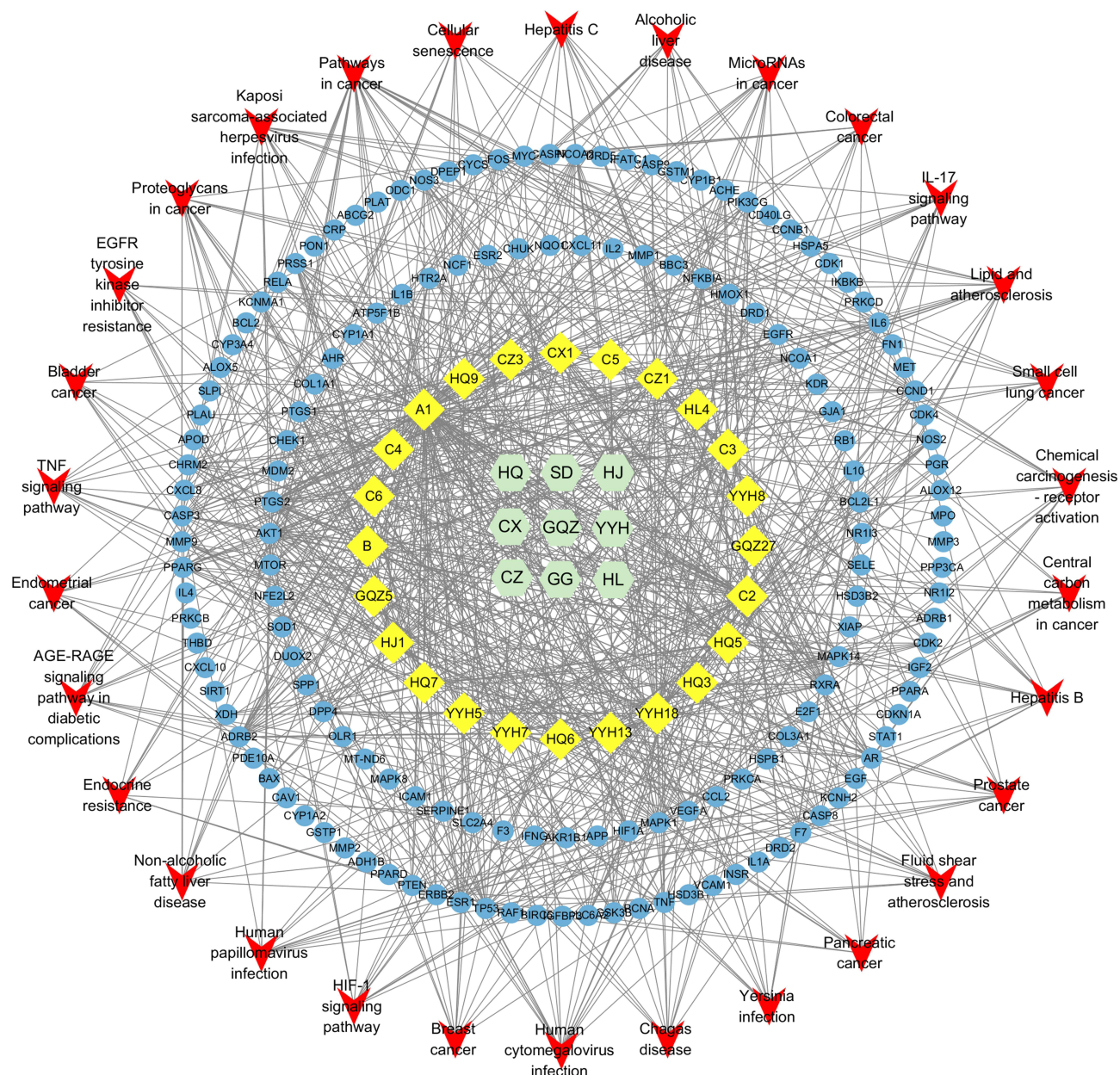


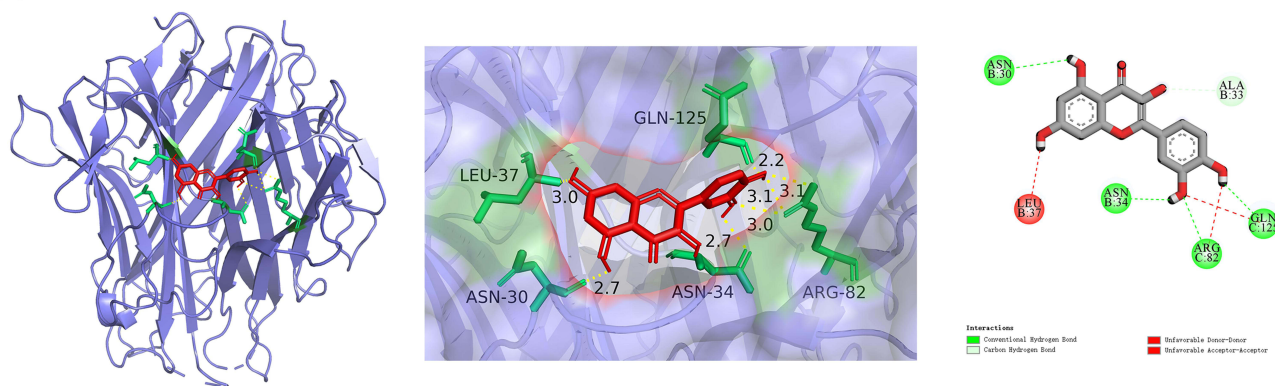
Figure 3 Drug-target-pathway Network. There were 9 drugs, 24 active compounds, 159 targets, and 30 signaling pathways in this network. Drugs are represented by hexagons, compounds by diamonds, targets by circles, and signaling pathways by arrows.

The HE results of rat kidney tissue showed that compared with the normal group, the glomerular mesangial matrix in the model group showed slight increase. The renal tubular epithelial cells expanded and showed vacuolar degeneration. The degree of renal tubular vacuolar degeneration was significantly reduced in the YQBS-H and the metformin group (Figure 6E).

Table 4 Results of Docking Between Key Targets and Active Compounds

Target	Compound	Binding energy(kcal mol ⁻¹)	Hydrogen bond
TNF	Quercetin	-6.5	Yes
TNF	Kaempferol	-8.8	Yes
IL6	Quercetin	-8.3	Yes

A



B

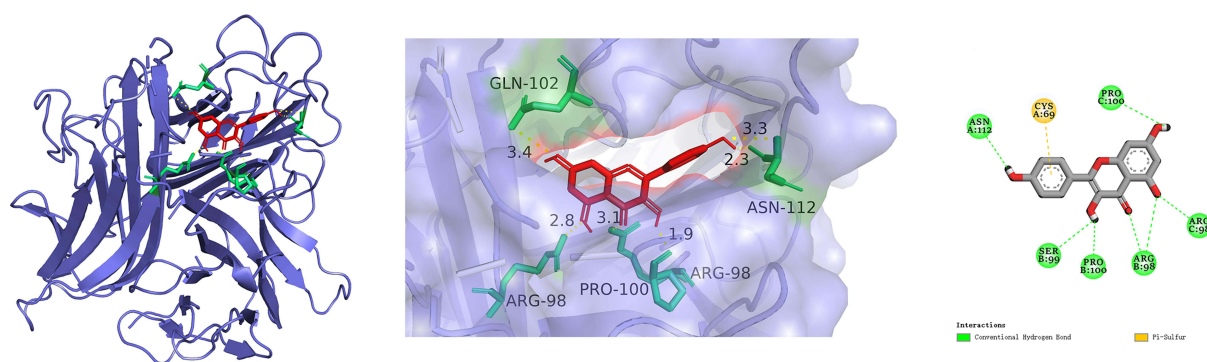


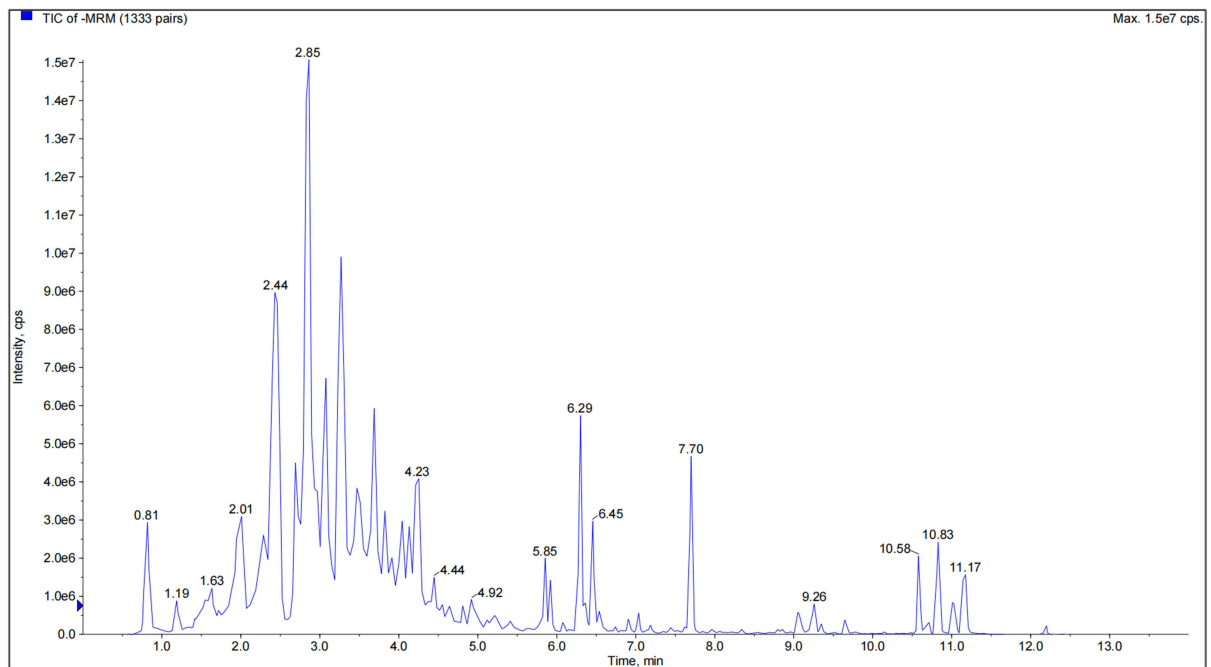
Figure 4 Molecular docking results. (A) Docking mode of TNF- α and quercetin. (B) Docking mode of TNF- α and kaempferol.

Meanwhile, YQBS significantly ameliorated the performance of rats in the MWM test. Compared to the DN group, the escape latency period in the treatment groups was significantly shortened (Figure 7A). In contrast with the Control group, the number of rats crossing the platform area in the DN group was reduced with statistical significance ($p < 0.01$), and the time spent in the target quadrant was shortened with statistical significance ($p < 0.001$). Conversely, in contrast with the DN group, the number of platform area crossings in the YQBS-H group increased ($p < 0.05$), and the time spent in the target quadrant was extended ($p < 0.001$) with statistical significance, as shown in Figure 7B and C. Figure 7D displays the swimming track diagram of each group of rats in the water maze.

YQBS Alleviated the Expression of TLR4/NF- κ B and Inflammatory Factors

YQBS might improve the pathological changes in the hippocampus of DN combined with CD through the TLR4/NF- κ B pathway (Figure 8A). Western blotting analysis of TLR4 (Figure 8B), NF- κ B p65 (Figure 8C), and phospho-NF- κ B p65 (Figure 8D) in the hippocampus revealed a significant reduction in the expressions of TLR4 as well as phospho-NF- κ B p65 in the hippocampus of YQBS-H group in contrast with the DN group ($p < 0.01$). Besides, the trend of changes in protein expression levels of TLR4/NF- κ B pathway in kidneys is consistent with that in hippocampus (Figure 8E–H). TLR4 as well as phospho-NF- κ B p65 in the kidneys of YQBS-H group in contrast with the DN group were also reduced significantly ($p < 0.01$ or $p < 0.001$). The expression of TLR4 and phospho-NF- κ B p65 in the YQBS-M and Metformin groups also decreased following treatments with YQBS as well as Metformin in contrast with the DN group ($p < 0.05$ or $p < 0.01$ or $p < 0.001$). Based on these results, it could be inferred that the TLR4/NF- κ B signaling pathway plays a crucial role in the anti-inflammatory effects of YQBS for DN accompanied with CD.

A



B

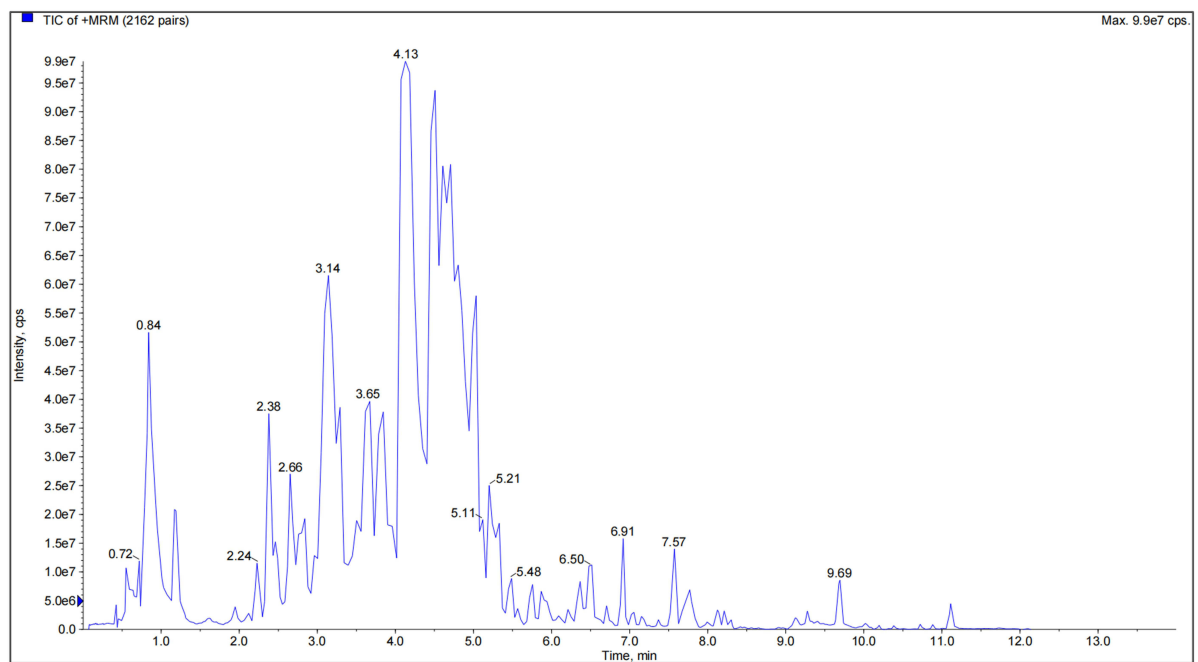


Figure 5 Analysis of the main chemical components of YQBS by UPLC-MS-MS. (A) Negative ion mode. (B) Positive ion mode.

Furthermore, ELISA results showed that the levels of TNF- α (Figure 8I) as well as IL-6 (Figure 8J) in serum were higher in the DN group in contrast with the Control group ($p < 0.001$). Following treatments with YQBS as well as Metformin, the levels of TNF- α alongside IL-6 in serum were reduced compared to the DN group ($p < 0.001$).

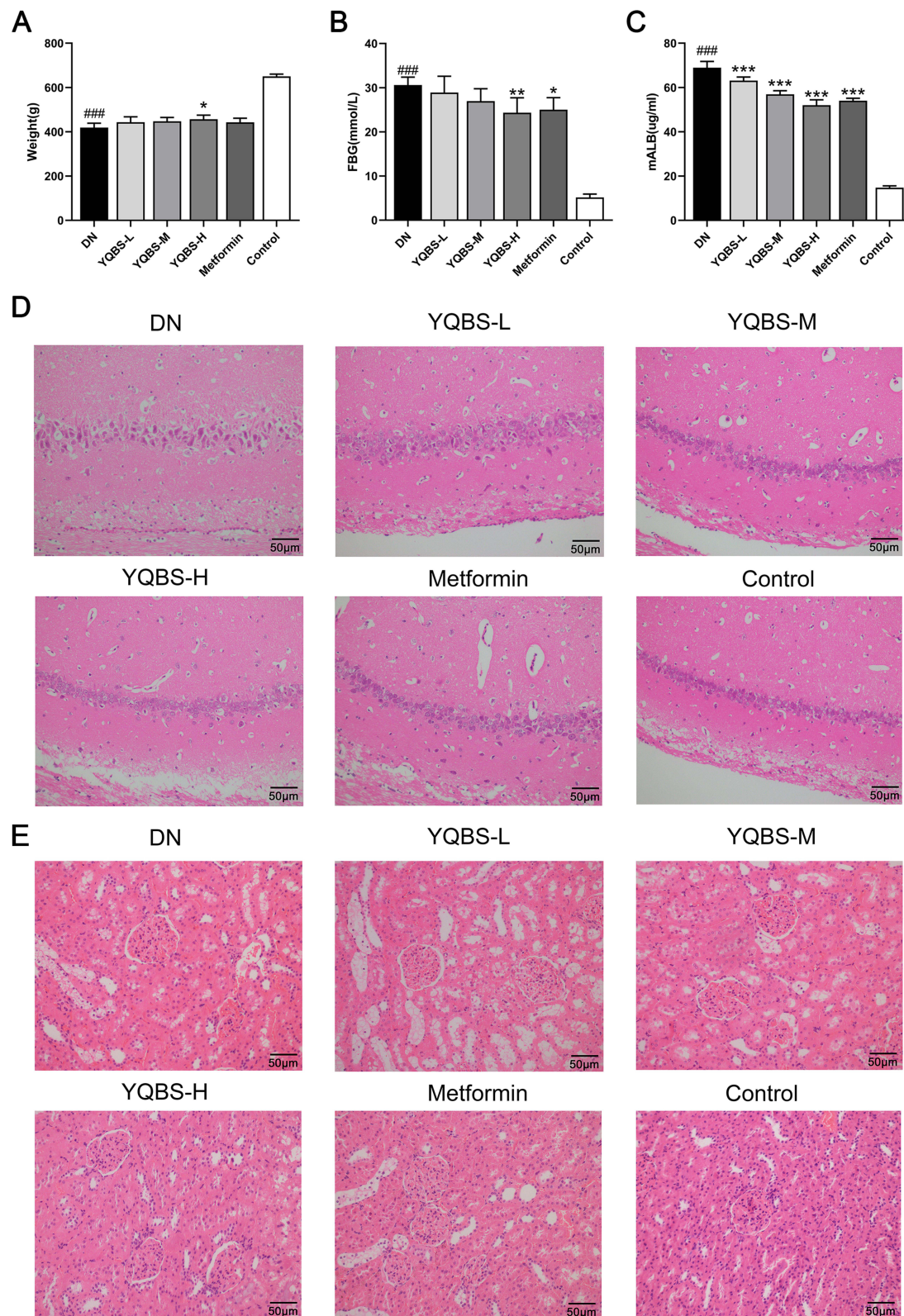


Figure 6 Experimental verification results in DN rats. **(A)** Analysis of body weight in each group of rats ($n = 6$). **(B)** Comparison of fasting blood glucose (FBG) levels among different groups of rats ($n = 6$). **(C)** Comparison of 24 h urinary mALB concentration in rats of each group ($n = 6$). **(D)** Representative morphological changes in the hippocampus of rats in each group (HE staining, 200 \times). **(E)** Representative morphological changes in the kidneys of rats in each group (HE staining, 200 \times). #### $p < 0.001$ compared to the Control; * $p < 0.05$, ** $p < 0.01$, and *** $p < 0.001$ compared to the DN.

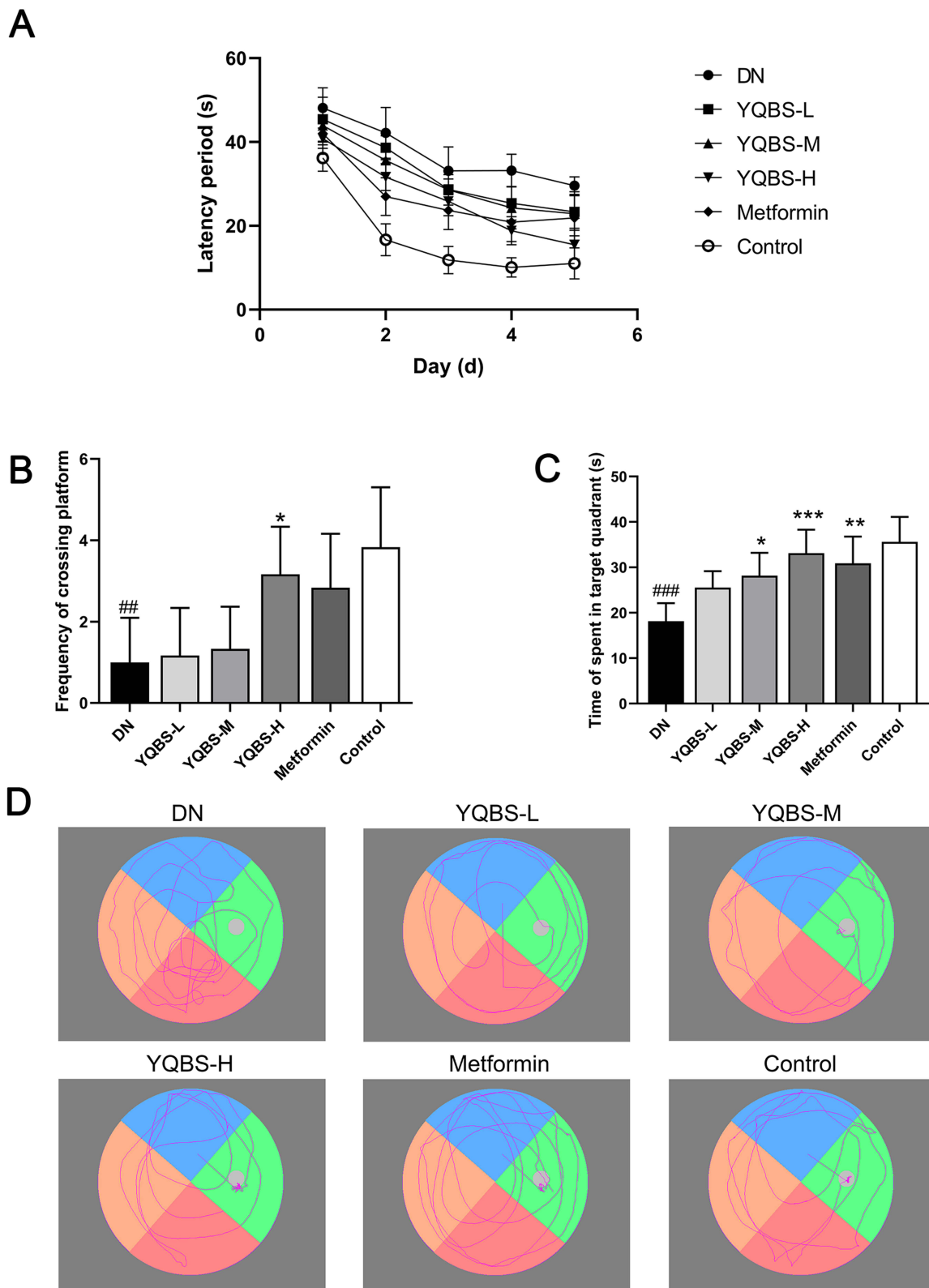


Figure 7 Comparison of MWM performance in each group. **(A)** Latency period in each group of rats. **(B)** Time spent in the target quadrant by each group of rats. **(C)** Frequency of crossing the platform by each group of rats. **(D)** Representative swimming track diagram of each group of rats. ###*p* < 0.01, and ####*p* < 0.001 compared to the Control; **p* < 0.05, ***p* < 0.01, and ****p* < 0.001 compared to the DN.

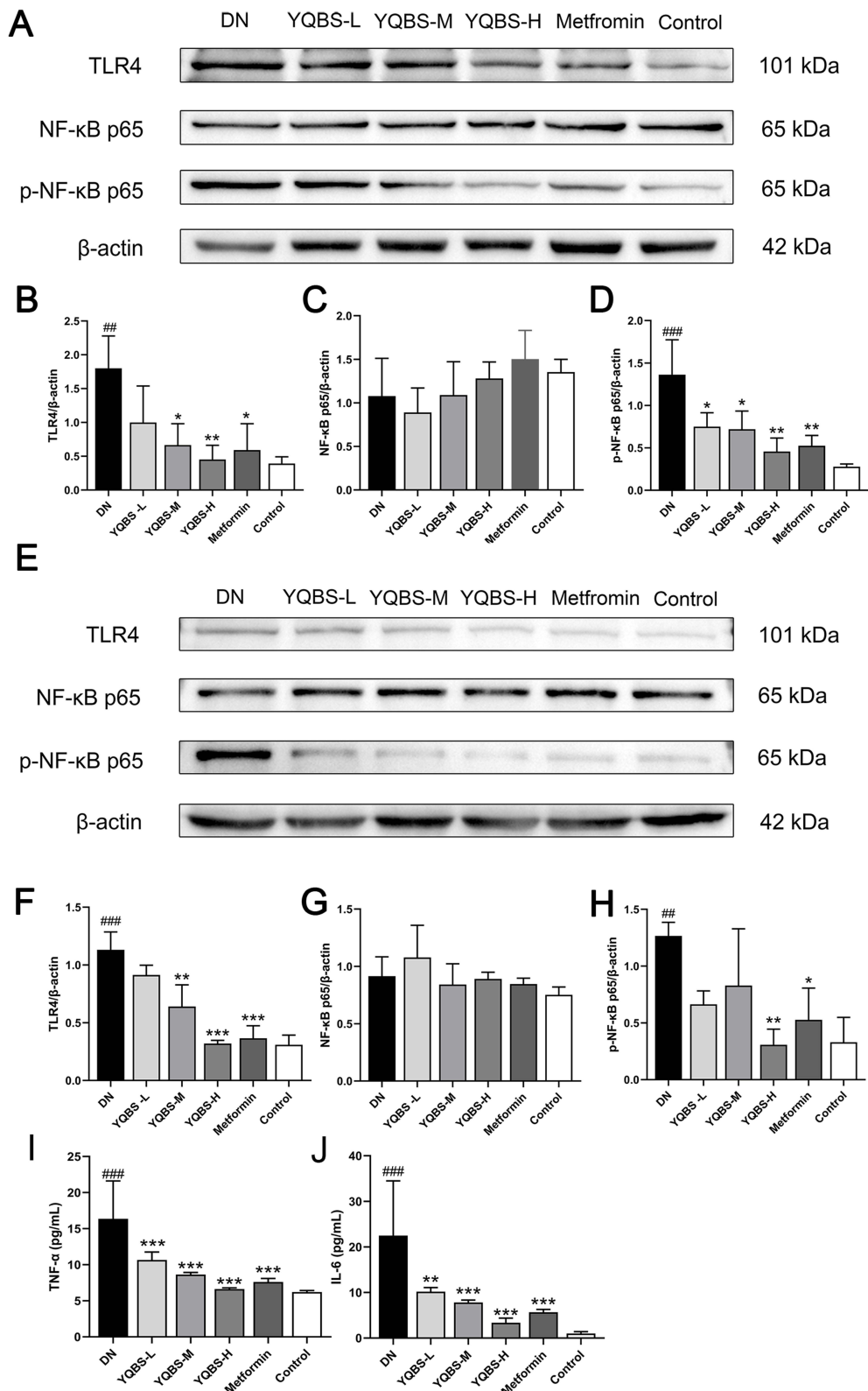


Figure 8 Expression of TLR4/NF-κB and inflammatory factors. (A) Protein expression levels of TLR4, NF-κB p65, and phospho-NF-κB p65 in hippocampal tissue were determined using Western blotting. (B) Relative quantitative analysis of hippocampal TLR4 expression. (C) Relative quantitative analysis of hippocampal NF-κB p65 expression. (D) Relative quantitative analysis of hippocampal phospho-NF-κB p65 expression. (E) Western blotting was used to detect the protein expression levels of TLR4, NF-κB p65, and phospho-NF-κB p65 in kidney tissue. (F) Relative quantitative analysis of kidney TLR4 expression. (G) Relative quantitative analysis of kidney NF-κB p65 expression. (H) Relative quantitative analysis of kidney phospho-NF-κB p65 expression. (I) Serum level of TNF-α. (J) Serum level of IL-6. ###*p* < 0.01, and ####*p* < 0.001 compared to the Control; **p* < 0.05, ***p* < 0.01, and ****p* < 0.001 compared to the DN.

Discussion

Modern medical research has highlighted a connection between DN and CD. In a group of middle-aged and elderly individuals with long-standing DM and a high risk of cardiovascular events, studies have shown that increased levels of albuminuria and cystatin C are closely related to poorer performance in processing speed tests. Additionally, albuminuria has been related to lower scores in verbal memory tests.⁸ Research has also suggested that retinol-binding protein (RBP4) could serve as a predictor of asymptomatic cerebral infarction in patients with DN, and it was found to be positively correlated with CD.⁴⁸ Furthermore, certain studies have explored the improvement of DN and CD through specific targets. For example, Esculin has been identified as a potential therapeutic agent that may improve DN with CD through the MAPK signaling pathway, exerting antioxidant stress, and demonstrating anti-inflammatory effects.⁴⁹ However, despite these advancements, the mechanism and therapeutic targets for CD in DN were not completely clear.

In TCM, there was not a specific term for DN and CD. However, based on clinical symptoms, they can be classified as “Xi Xiao” within the context of “Xiao Ke” which combines features of “Da Bing” and “Jian Wang”. YQBS has shown efficacy in treating DM and its complications of kidney qi deficiency. The recipe includes 9 herbs, and there are 2 sovereign herbs. HQ replenishes qi and raises yang; SD tonifies the kidney, generates essence, and nourishes yin and blood. In TCM theory, the brain is considered the “medullary sea” and adequate kidney essence nourishment is essential for brain health. HJ, GQZ, and CX serve as minister herbs. HJ nourishes yin and qi, tonifies the kidney and essence; GQZ nourishes the liver and kidney, strengthens essence and yang, nourishes blood and promotes fluid production; CX ascends the head, helps lucid yang, promotes blood circulation and unblocking collaterals. YYH, GG, HL and CZ serve as assistant herbs. YYH complements HQ in replenishing qi, and helps HJ and SD in tonifying the kidney; GG and HL can clear heat and detoxify, and they can amplify the effects of tonifying qi and kidney, fortifying the brain, as well as clearing turbidity while detoxifying; CZ functions to dry and invigorate the spleen, promoting the circulation of qi to prevent the greasiness, additionally, it aids in clearing and eliminating stasis caused by phlegm retention. In brief, YQBS tonifies qi and kidney, strengthens the brain and marrow, promotes blood circulation, and detoxifies turbidity. Previous research has demonstrated that YQBS can regulate glucose and lipid metabolism, reduce insulin resistance, and delay the onset and progression of DM and its complications.

The network pharmacology analysis revealed that YQBS contains active ingredients such as quercetin, kaempferol, β -sitosterol, formononetin, stigmaterol, luteolin, and others, which could be used to treat DN combined with CD. Quercetin and kaempferol, both flavonoids, are known for their anti-inflammatory as well as antioxidant properties.^{50–53} Quercetin has been shown to have various effects such as anti-hyperglycemia, anti-oxidative stress, and anti-inflammation, which can help improve both DN and CD.^{54–57} Studies have indicated that quercetin can impact targets and pathways like TNF- α , NF- κ B, and AKT, leading to benefits such as reduced blood glucose levels, increased insulin sensitivity, facilitating the treatment and prevention of DM and its complications.⁵⁸ Kaempferol, on the other hand, may offer protective effects against DN by alleviating inflammation, reducing cell apoptosis, and enhancing podocyte autophagy.^{59,60} It can also potentially impact CD through its antioxidant properties.⁶¹ Some research suggests that kaempferol may inhibit TRK β mediated by the N-methyl-D-aspartate receptor outside the hippocampal synapse thereby improving CD.⁶²

PPI network analysis revealed that the core targets were AKT1, TNF, IL-6, TP53, and VEGFA. The enrichment analysis of GO and KEGG pathways suggested that the mechanism of YQBS in treating DN with CD might be mainly related to Human cytomegalovirus infection, the HIF-1 signaling pathway, the NF- κ B signaling pathway, and other associated signaling pathways. The main BPs were positive regulation of gene expression, angiogenesis, and cellular response to hypoxia. TNF and IL-6 were included in 58 and 47 pathways, respectively. The results of molecular docking indicated that TNF and IL-6 had certain binding activity with key components such as quercetin and kaempferol, forming hydrogen bonds. These complexes could be the primary active compounds in YQBS for treating DN with CD. The results of network pharmacology indicated that IL-6 and TNF- α were potential targets of YQBS in the treatment of DN combined with CD. Human cytomegalovirus infection, the HIF-1 signaling pathway, as well as the NF- κ B signaling pathway were identified as important signaling pathways. TLR4, NF- κ B, IL-6, and TNF- α were implicated in Human cytomegalovirus infection, HIF-1 signaling pathway, and NF- κ B signaling pathway.

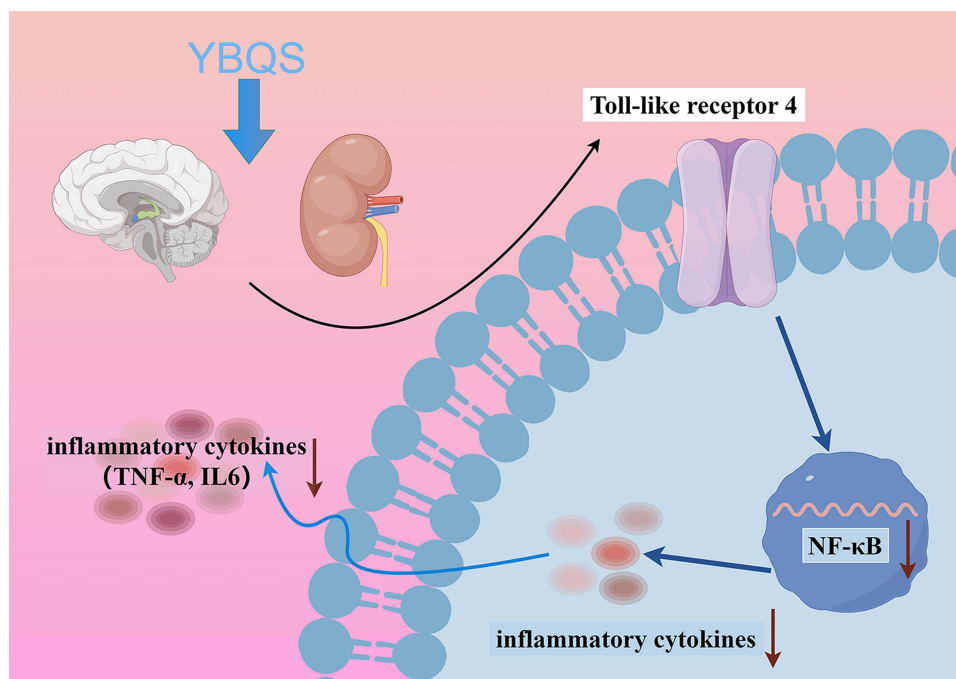


Figure 9 The mechanism diagram of YQBS alleviating DN with CD.

Inflammation plays a very important role in the occurrence and development of DN and CD.^{63,64} The NF- κ B signaling pathway is a significant inflammatory pathway closely related to the occurrence and development of DN.⁶⁵ TNF- α and IL-6 are essential cytokines involved in the body's metabolic processes. Certain drugs that improved DN and CD can significantly inhibit the expression of TNF- α and IL-6 in the kidneys, brain, and blood of rats, as well as reduce inflammatory cell infiltration, indicating that TNF and IL-6 are crucial targets for relieving DN and CD.^{66–69} TLR4 is widely present in podocytes and microglia. TLR4 could activate NF- κ B when in a quiescent state. The activated NF- κ B p65 can regulate the expression of various inflammatory factors, including TNF- α , IL-6, and other factors, thereby inducing inflammatory responses and exacerbating DN and central nervous system diseases such as cognitive impairment.^{70–73} The results from network pharmacology indicated that the key targets and pathway of YQBS in treating DN combined with CD are TNF- α , IL-6, as well as the NF- κ B pathway. Therefore, we investigated whether YQBS could mitigate inflammation through the TLR4/NF- κ B signaling pathway via animal experimental validation. The animal experimental validation results showed that YQBS could enhance renal and cognitive function in DN rats. Compared to the DN group, the expressions of TLR4, NF- κ B, TNF- α , and IL-6 in the kidneys and hippocampus of the YQBS group were significantly decreased. This study suggests that YQBS may act through the TLR4/NF- κ B pathway, influencing the expressions of TNF- α alongside IL-6. YQBS may reduce inflammation through this pathway, thereby alleviating DN complicated with CD (Figure 9).

This study provided a basis for further investigations into the anti-inflammatory effects of YQBS on both kidney and hippocampal tissues. It represented a breakthrough in elucidating the therapeutic basis and pharmacological mechanism of TCM in the treatment of DN with CD, offering insights and a research foundation for future research on the “Kidney-Brain Axis”. However, this study had some limitations. Some targets of DN and CD may not be currently included in public databases. The results demonstrated that YQBS could improve DN with CD in rats. However, further research is necessary to fully understand the underlying mechanism.

Conclusion

YQBS and its active ingredients have been shown to have positive effects in the treatment of diabetes and its complications. Network pharmacology analyses and experimental validation have indicated quercetin and kaempferol, two important components of YQBS, as the main contributors to its anti-inflammatory activity, and the mechanism

underlying its anti-inflammatory effects may involve TLR4/NF- κ B signaling pathway. These findings provide basis and ideas for the future research and development of YQBS, which could help alleviate the pressure on patients suffering from diabetic complications. The present research lays a theoretical foundation and insights for future experimental investigations and clinical practice. Additionally, it has provided significant progress in elucidating the pharmacological basis and mechanism of traditional Chinese medicine in inflammatory-induced diabetic complications.

Data Sharing Statement

Data is contained within the article.

Ethical Approval and Consent to Participate

Ethical approval to conduct studies using publicly available databases is exempt under the following legislation:

Item 1 and 2 of Article 32 of “the Measures for Ethical Review of Life Science and Medical Research Involving Human Subjects”, which was reviewed by the National Science and Technology Ethics Committee, approved by the State Council of China, and jointly promulgated by the National Health Commission, the Ministry of Education, the Ministry of Science and Technology and the State Administration of Traditional Chinese Medicine on Feb. 18, 2023.

This study was conducted in accordance with the ARRIVE guidelines for in vivo experiments. This study was approved by the Experimental Animal Ethics Committee of Qilu Hospital of Shandong University (DWLL-2022-073) following the guidelines for the ethical review of laboratory animal welfare People’s Republic of China National Standard GB/T 35892-2018.

Funding

This study was supported by the Qilu Geriatric Diseases Chinese and Western Academic School Inheritance Workshop Project (No. 2022-93-1-10).

Disclosure

The authors declare that they have no conflicts of interest in this study.

References

1. Pearson ER. Type 2 diabetes: a multifaceted disease. *Diabetologia*. 2019;62:1107–1112. doi:10.1007/s00125-019-4909-y
2. Bloomgarden ZT. Diabetic nephropathy. *Diabetes Care*. 2005;28:745–751. doi:10.2337/diacare.28.3.745
3. Natesan V, Kim S. Diabetic nephropathy - a review of risk factors, progression, mechanism, and dietary management. *Biomol Ther*. 2021;29:365–372. doi:10.4062/biomolther.2020.204
4. Miles WR, Root HF. Psychologic tests applied to diabetic patients. *Arch Intern Med*. 1922;30:767–777. doi:10.1001/archinte.1922.00110120086003
5. Hu ZX, Jiao R, Wang PP, et al. Shared Causal Paths underlying Alzheimer’s dementia and Type 2 Diabetes. *Sci Rep*. 2020;10(1):4107. doi:10.1038/s41598-020-60682-3
6. Koekkoek PS, Kappelle LJ, Berg E, et al. Cognitive function in patients with diabetes mellitus: guidance for daily care. *Lancet Neurol*. 2015;14:329–340. doi:10.1016/S1474-4422(14)70249-2
7. Zhang JY, Chen CX, Hua SZ, et al. An updated meta-analysis of cohort studies: diabetes and risk of Alzheimer’s disease. *Diabet Res Clin Pract*. 2017;124:41–47. doi:10.1016/j.diabres.2016.10.024
8. Murray AM, Barzilay JI, Lovato JF, et al. Biomarkers of renal function and cognitive impairment in patients with diabetes. *Diabetes Care*. 2011;34:1827–1832. doi:10.2337/dc11-0186
9. McCarthy I. The physiology of bone blood flow: a review. *J Bone Joint Surg Am*. 2006;88(3):4–9.
10. Mogi M, Horiuchi M, Aihara KI. Clinical interaction between brain and kidney in small vessel disease. *Cardiol Res Pract*. 2011;306185–306189.
11. Barzilay JI, Lovato JF, Murray AM, et al. Albuminuria and cognitive decline in people with diabetes and normal renal function. *Clin J Am Soc Nephrol*. 2013;8:1907–1914. doi:10.2215/CJN.11321112
12. Barzilay JI, Gao P, O’Donnell M, et al. Albuminuria and decline in cognitive function: the ONTARGET/TRANSCEND studies. *Arch Intern Med*. 2011;171:142–150. doi:10.1001/archinternmed.2010.502
13. Li JL, Jin CH, Cleveland JJ, et al. Enhanced inflammatory responses to toll-like receptor 2/4 stimulation in type 1 diabetic coronary artery endothelial cells: the effect of insulin. *Cardiovasc Diabetol*. 2010;9:90. doi:10.1186/1475-2840-9-90
14. Lin M, Yiu WH, Li RX, et al. The TLR4 antagonist CRX-526 protects against advanced diabetic nephropathy. *Kidney Int*. 2013;83:887–900. doi:10.1038/ki.2013.11
15. Vitseva OI, Tanriverdi K, Tchkonja TT, et al. Inducible Toll-like Receptor and NF- κ B regulatory pathway expression in human adipose tissue. *Obesity*. 2008;16:932–937. doi:10.1038/oby.2008.25

16. Yang MX, Gan H, Shen Q, Tang WX, Du XG, Chen DY. Proinflammatory CD14+CD16+ monocytes are associated with microinflammation in patients with type 2 diabetes mellitus and diabetic nephropathy uremia. *Inflammation*. 2012;35(1):388–396. doi:10.1007/s10753-011-9374-9
17. Liao H, Hu L, Cheng XN, et al. Are the therapeutic effects of Huangqi (*Astragalus membranaceus*) on diabetic nephropathy correlated with its regulation of macrophage iNOS activity? *J Immunol Res*. 2017;2017:3780572–3780579. doi:10.1155/2017/3780572
18. Chen HY, Zhu Q, Tang XL, Min M, Jie LQ, Chen LJ. Effect of Shen-qi-di-huang decoction on reducing proteinuria by preserving nephrin in Adriamycin-induced nephropathy rats. *Afr J Tradit Complement Altern Med*. 2011;8:467–476. doi:10.4314/ajtcam.v8i4.20
19. Di S, Han L, Wang Q, et al. A network pharmacology approach to uncover the mechanisms of Shen-Qi-Di-Huang decoction against diabetic nephropathy. *Evid Based Compl Alternat Med*. 2018;7043402–7043414. doi:10.1155/2018/7043402
20. Du XM, Pan W, Liang YL, Zhang Q. Observation on the curative effect of modified Shenqi Dihuang decoction in treating diabetic kidney disease with deficiency of both Qi and Yin and its effects on intestinal flora and inflammation factors. *Trad Chin Drug Res Clin Pharm*. 2021;32:566–572. Chinese.
21. Wang KS 2020. Meta analysis of the clinical efficacy of Shen-qi-Di-huang decoction in the prevention and treatment of diabetes kidney disease [master's thesis]. Shenyang (Liaoning): Liaoning University of Traditional Chinese Medicine.
22. Ning LN 2021. Protective effect and mechanism of the Chinese Yi-Qi-Bu-Shen recipe on kidney injury in diabetic mice [master's thesis], Jinan (Shandong): Shandong University of Traditional Chinese Medicine.
23. Liu DS, Lin WW, Gao W, Chang P, Li W. Effect of Yiqi Bushen prescription on hippocampal neuronal apoptosis in diabetic rats. *Neural Regeneration Res*. 2011;6:1628–1634.
24. Liu DS, Wang SL, Zhang JD. Clinical study on diabetic brain dysfunction syndrome treated with Naoshenkang. *J Nanjing Univ of Trad Chin Med*. Vol. 21;2005:95–97. Chinese.
25. Liu XH 2020. Preventive effect and mechanism of Yiqi Bushen recipe on kidney injury and fibrosis in diabetic mice [master's thesis]. Jinan (Shandong): Shandong University of Traditional Chinese Medicine.
26. Zhang X 2019. Study on the Mechanism of delaying renal lesion in diabetes mice with Yi-Qi-Bu-Shen recipe by down-regulating lncRNANONMMUT066973 [master's thesis]. Jinan (Shandong): Shandong University.
27. Liu DS, Zhou YH, Liang ES, et al. Neuroprotective effects of the Chinese Yi-Qi-Bu-Shen recipe extract on injury of rat hippocampal neurons induced by hypoxia/reoxygenation. *J Ethnopharmacol*. 2013;145:168–174. doi:10.1016/j.jep.2012.10.046
28. Liu YZ, Cai JR, Wang YG, Zhao XL, Qiao Y, Liu CJ. YQBS improves cognitive dysfunction in diabetic rats: possible association with tyrosine and tryptophan metabolism. *Diabet Metab Syndr Obes*. 2023;16:901–912. doi:10.2147/DMSO.S401863
29. Ru JL, Li P, Wang JN, et al. TCMSP: a database of systems pharmacology for drug discovery from herbal medicines. *J Cheminform*. 2014;6:13. doi:10.1186/1758-2946-6-13
30. Huang C, Zheng CL, Li Y, Wang YH, Lu A, Yang L. Systems pharmacology in drug discovery and therapeutic insight for herbal medicines. *Brief Bioinform*. 2014;15:710–733. doi:10.1093/bib/bbt035
31. Feng WW, Ao H, Yue SJ, Peng C. Systems pharmacology reveals the unique mechanism features of Shenzhu Capsule for treatment of ulcerative colitis in comparison with synthetic drugs. *Sci Rep*. 2018;8(1):16160. doi:10.1038/s41598-018-34509-1
32. Consortium TU. UniProt: a worldwide hub of protein knowledge. *Nucleic Acids Res*. 2019;47(D1):D506–D515.
33. Amberger JS, Hamosh A. Searching Online Mendelian Inheritance in Man (OMIM): a Knowledgebase of Human Genes and Genetic Phenotypes. *Curr Protoc Bioinformatics*. 2017;58(1):1–2. doi:10.1002/cpbi.27
34. Stelzer G, Rosen N, Plaschkes I, et al. The GeneCards Suite: from Gene Data Mining to Disease Genome Sequence Analyses. *Curr Protoc Bioinformatics*. 2016;54(1):1–30. doi:10.1002/cpbi.5
35. Wishart DS, Feunang YD, Guo AC, et al. DrugBank 5.0: a major update to the DrugBank database for 2018. *Nucleic Acids Res*. 2018;46(D1):D1074–D1082. doi:10.1093/nar/gkx1037
36. Pinero J, Ramirez-Angueta JM, Sauch-Pitarch J, et al. The DisGeNET knowledge platform for disease genomics: 2019 update. *Nucleic Acids Res*. 2020;48(D1):D845–D855. doi:10.1093/nar/gkz1021
37. Wang YX, Zhang S, Li FC, et al. Therapeutic target database 2020: enriched resource for facilitating research and early development of targeted therapeutics. *Nucleic Acids Res*. 2020;48(D1):D1031–D1041.
38. Szklarczyk D, Gable AL, Lyon D, et al. STRING v11: protein–protein association networks with increased coverage, supporting functional discovery in genome-wide experimental datasets. *Nucleic Acids Res*. 2019;47(D1):D607–D613. doi:10.1093/nar/gky1131
39. Shi HS, Dong CD, Wang M, et al. Exploring the mechanism of Yizhi Tongmai decoction in the treatment of vascular dementia through network pharmacology and molecular docking. *Ann Transl Med*. 2021;9:164. doi:10.21037/atm-20-8165
40. Huang DW, Sherman BT, Lempicki RA. Systematic and integrative analysis of large gene lists using DAVID bioinformatics resources. *Nat Protoc*. 2009;4(1):44–57. doi:10.1038/nprot.2008.211
41. Zhou YY, Zhou B, Pache L, et al. Metascape provides a biologist-oriented resource for the analysis of systems-level datasets. *Nat Commun*. 2019;10(1):1523.
42. Kim S, Thiessen PA, Bolton EE, et al. PubChem Substance and Compound databases. *Nucleic Acids Res*. 2016;44(D1):D1202–D1213. doi:10.1093/nar/gkv951
43. Berman HM, Westbrook J, Feng Z, et al. The Protein Data Bank. *Nucleic Acids Res*. 2000;28(1):235–242. doi:10.1093/nar/28.1.235
44. Trott O, Olson AJ. AutoDock Vina: improving the speed and accuracy of docking with a new scoring function, efficient optimization, and multithreading. *J Comput Chem*. 2010;31:455–461. doi:10.1002/jcc.21334
45. Zhong LH, Zhao Y, Liu DS. [Quality control of invigorating Qi and tonifying kidney “NaoShenKang” Capsule]. *J Shandong Univ*. 2010;48:116–119. Chinese.
46. El-Nasr NME A, Saleh DO, Hashad IM. Role of olmesartan in ameliorating diabetic nephropathy in rats by targeting the AGE/PKC, TLR4/P38-MAPK and SIRT-1 autophagic signaling pathways. *Eur J Pharmacol*. 2022;928:175117. doi:10.1016/j.ejphar.2022.175117
47. Ying C, Mao Y, Chen L, et al. Bamboo leaf extract ameliorates diabetic nephropathy through activating the AKT signaling pathway in rats. *Int J Biol Macromol*. 2017;105:1587–1594. doi:10.1016/j.ijbiomac.2017.03.124
48. Chen DY, Huang XL, Lu S, et al. RBP4/Lp-PLA2/Netrin-1 signaling regulation of cognitive dysfunction in diabetic nephropathy complicated with silent cerebral infarction. *Exp Clin Endocrinol Diabetes*. 2017;125:547–553. doi:10.1055/s-0043-109099

49. Song Y, Wang XC, Qin SK, Zhou SH, Li JL, Gao Y. Esculin ameliorates cognitive impairment in experimental diabetic nephropathy and induces anti-oxidative stress and anti-inflammatory effects via the MAPK pathway. *Mol Med Rep.* 2018;17:7395–7402. doi:10.3892/mmr.2018.8727
50. Devi KP, Malar DS, Nabavi SF, et al. Kaempferol and inflammation: from chemistry to medicine. *Pharmacolo Res.* 2015;99:1–10. doi:10.1016/j.phrs.2015.05.002
51. Feng K, Chen ZX, Liu PC, Zhang SH, Wang XQ. Quercetin attenuates oxidative stress-induced apoptosis via SIRT1/AMPK-mediated inhibition of ER stress in rat chondrocytes and prevents the progression of osteoarthritis in a rat model. *J Cell Physiol.* 2019;234:18192–18205. doi:10.1002/jcp.28452
52. Shen P, Lin WJ, Deng X, et al. Potential implications of quercetin in autoimmune diseases. *Front Immunol.* 2021;12:689044. doi:10.3389/fimmu.2021.689044
53. Simunkova M, Alwasel SH, Alhazza IM, et al. Management of oxidative stress and other pathologies in Alzheimer's disease. *Arch Toxicol.* 2019;93:2491–2513. doi:10.1007/s00204-019-02538-y
54. Bardestani A, Ebrahimpour S, Esmaili A, Esmaili A. Quercetin attenuates neurotoxicity induced by iron oxide nanoparticles. *J Nanobiotechnology.* 2021;19(1):327.
55. Ebrahimpour S, Shahidi SB, Abbasi M, Tavakoli Z, Esmaili A. Quercetin-conjugated superparamagnetic iron oxide nanoparticles (QCSPIONs) increases Nrf2 expression via miR-27a mediation to prevent memory dysfunction in diabetic rats. *Sci Rep.* 2020;10(1):15957. doi:10.1038/s41598-020-71971-2
56. Hu TY, Yue JL, Tang QW, et al. The effect of quercetin on diabetic nephropathy (DN): a systematic review and meta-analysis of animal studies. *Food Funct.* 2022;13:4789–4803. doi:10.1039/D1FO03958J
57. Swain SK, Chandra Dash U, Sahoo AK. Hydroleia zeylanica improves cognitive impairment in high-fat diet fed-streptozotocin-induced diabetic encephalopathy in rats via regulating oxidative stress, neuroinflammation, and neurotransmission in brain. *Heliyon.* 2022;8:e11301.
58. Yan L, Vaghari-Tabari M, Malakoti F, et al. Quercetin: an effective polyphenol in alleviating diabetes and diabetic complications. *Crit Rev Food Sci Nutr.* 2023;63(28):9163–9186. doi:10.1080/10408398.2022.2067825
59. Hu QC, Qu CY, Xiao XL, et al. Flavonoids on diabetic nephropathy: advances and therapeutic opportunities. *Chin Med.* 2021;16(1):74.
60. Sheng HQ, Zhang D, Zhang JQ, et al. Kaempferol attenuated diabetic nephropathy by reducing apoptosis and promoting autophagy through AMPK/mTOR pathways. *Front Med.* 2022;9:986825. doi:10.3389/fmed.2022.986825
61. Hosseini Z, Mansouritorghabeh F, Kakhki F, et al. Effect of Sanguisorba minor on scopolamine-induced memory loss in rat: involvement of oxidative stress and acetylcholinesterase. *Metab Brain Dis.* 2022;37:473–488. doi:10.1007/s11011-021-00898-y
62. Das D, Biswal S, Barhwal KK, Chaurasia OP, Hota SK. Kaempferol inhibits extra-synaptic NMDAR-mediated downregulation of TRKβ in rat hippocampus during hypoxia. *Neuroscience.* 2018;392:77–91. doi:10.1016/j.neuroscience.2018.09.018
63. Li HD, You YK, Shao BY, et al. Roles and crosstalks of macrophages in diabetic nephropathy. *Front Immunol.* 2022;13:1015142. doi:10.3389/fimmu.2022.1015142
64. Yin Q, Ma J, Han X, et al. Spatiotemporal variations of vascular endothelial growth factor in the brain of diabetic cognitive impairment. *Pharmacol Res.* 2021;163:105234. doi:10.1016/j.phrs.2020.105234
65. Mezzano S, Aros C, Droguett A, et al. NF-kappaB activation and overexpression of regulated genes in human diabetic nephropathy. *Nephrol Dial Transplant.* 2004;19:2505–2512. doi:10.1093/ndt/gfh207
66. Bai LT, Gao JL, Wei F, Zhao J, Wang DW, Wei J. Therapeutic potential of ginsenosides as an adjuvant treatment for diabetes. *Front Pharmacol.* 2018;9:423. doi:10.3389/fphar.2018.00423
67. Malik S, Suchal K, Khan SI, et al. Apigenin ameliorates streptozotocin-induced diabetic nephropathy in rats via MAPK-NF-κB-TNF-α and TGF-β1-MAPK-fibronectin pathways. *Am J Physiol Renal Physiol.* 2017;313:F414–F422. doi:10.1152/ajprenal.00393.2016
68. Xiang E, Han B, Zhang Q, et al. Human umbilical cord-derived mesenchymal stem cells prevent the progression of early diabetic nephropathy through inhibiting inflammation and fibrosis. *Stem Cell Res Ther.* 2020;11(1):336. doi:10.1186/s13287-020-01852-y
69. Xie ZP, Lu H, Yang SX, et al. Salidroside attenuates cognitive dysfunction in senescence-accelerated mouse prone 8 (SAMP8) mice and modulates inflammation of the Gut-Brain axis. *Front Pharmacol.* 2020;11:568423. doi:10.3389/fphar.2020.568423
70. Leitner GR, Wenzel TJ, Marshall N, Gates EJ, Klegeris A. Targeting toll-like receptor 4 to modulate neuroinflammation in central nervous system disorders. *Expert Opin Ther Targets.* 2019;23:865–882. doi:10.1080/14728222.2019.1676416
71. García Bueno B, Caso JR, Madrigal JL, Leza JC. Innate immune receptor Toll-like receptor 4 signalling in neuropsychiatric diseases. *Neurosci Biobehav Rev.* 2016;64:134–147. doi:10.1016/j.neubiorev.2016.02.013
72. Verzola D, Cappuccino L, D'Amato E, et al. Enhanced glomerular Toll-like receptor 4 expression and signaling in patients with type 2 diabetic nephropathy and microalbuminuria. *Kidney Int.* 2014;86:1229–1243. doi:10.1038/ki.2014.116
73. Qi MY, He YH, Cheng Y, et al. Icarin ameliorates streptozotocin-induced diabetic nephropathy through suppressing the TLR4/NF-κB signal pathway. *Food Funct.* 2021;12:1241–1251. doi:10.1039/D0FO02335C

Diabetes, Metabolic Syndrome and Obesity

Dovepress

Publish your work in this journal

Diabetes, Metabolic Syndrome and Obesity is an international, peer-reviewed open-access journal committed to the rapid publication of the latest laboratory and clinical findings in the fields of diabetes, metabolic syndrome and obesity research. Original research, review, case reports, hypothesis formation, expert opinion and commentaries are all considered for publication. The manuscript management system is completely online and includes a very quick and fair peer-review system, which is all easy to use. Visit <http://www.dovepress.com/testimonials.php> to read real quotes from published authors.

Submit your manuscript here: <https://www.dovepress.com/diabetes-metabolic-syndrome-and-obesity-journal>